



ISTITUTO NAZIONALE
DI GEOFISICA E VULCANOLOGIA

Quantifying the ground displacement's acceleration by using the Failure Forecast Method during the **ongoing** unrest of Vulcano (Italy) in 2021-2022.

Andrea Bevilacqua⁽¹⁾, Valentina Bruno⁽²⁾, Mario Mattia⁽²⁾, Massimo Rossi⁽²⁾, Mauro Coltelli⁽²⁾, Augusto Neri⁽¹⁾

(1) *Istituto Nazionale di Geofisica e Vulcanologia, Sezione di Pisa, Italia*

(2) *Istituto Nazionale di Geofisica e Vulcanologia, Sezione di Catania – Osservatorio Etneo, Catania, Italia*



Cities on Volcanoes 11, Heraklion, Greece, June 15th 2022

Session 1.10 - Volcano monitoring and eruption forecasting in the presence of uncertainty



The ongoing 2021-2022 unrest crisis of Vulcano (Italy)

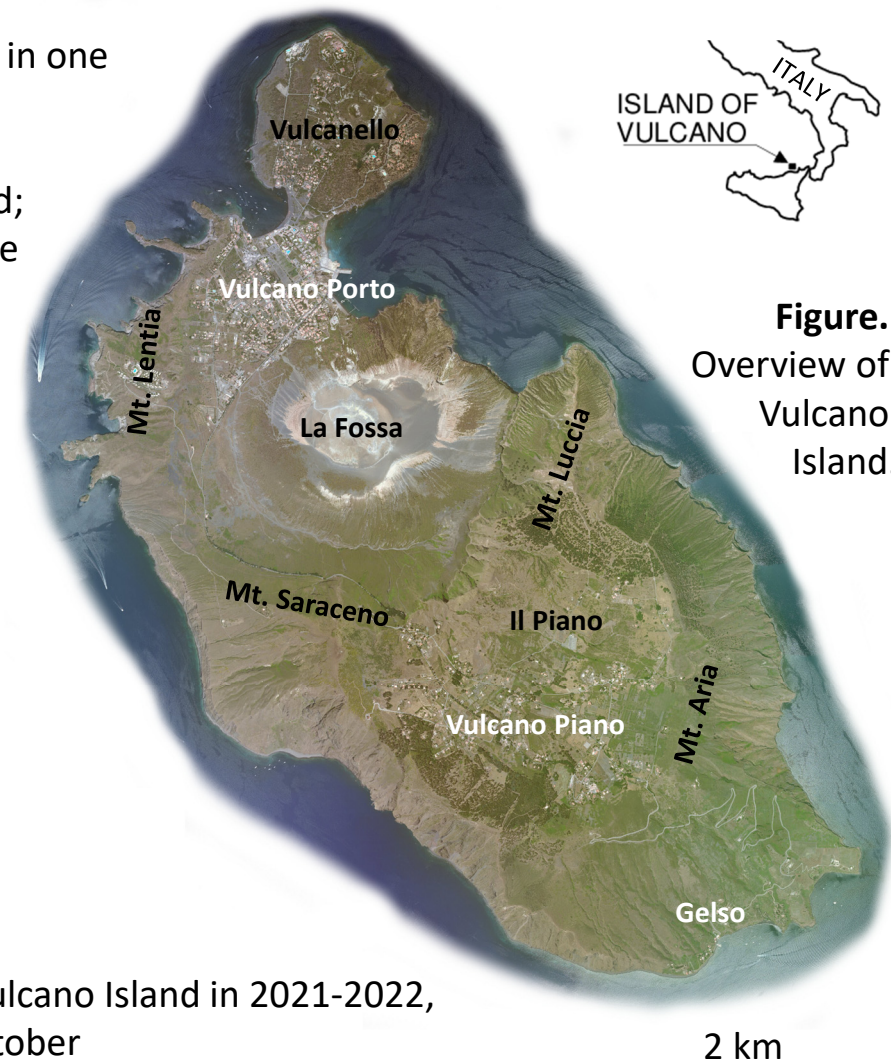
Since **September 2021**, a significant increase of unrest signals occurred, in particular:

- permanent GPS network measured an **accelerated inflation** of the La Fossa cone, ~2 cm in one month, peaking around October 10th
- **volcanic degassing** from the main fumarolic field on the La Fossa crater rapidly increased; diffuse CO₂ degassing, i.e. outside the fumarolic fields, grew up by one order of magnitude
- low energy **local seismicity** sharply increased, including VLP events, never recorded in the last 15 years since the broadband network installation.

In **October 2021**, the **diffuse degassing** impacted some areas far from the crater. Dipartimento della Protezione Civile increased the volcanic alert level to yellow, i.e. "Minor/shallow hydrothermal crisis".

Most geochemical parameters **continued** their increase until **November 2021** and they have not decreased since then (May 2022).

In this study, we analyze the **temporal rates of GPS data** collected by INGV network on Vulcano Island in 2021-2022, focusing on the mathematical properties of the rapid inflation occurred in September-October and of the 7-month long period afterwards.



Applying the Failure Forecast Method to track the unrest of Vulcano

The **Failure Forecast Method** (FFM) estimates the time at which the system of Vulcano may **enter a critical state**, under the assumption that the nonlinear trend of the signals observed in the previous weeks will continue in the future, and accelerate in the same way as **brittle materials** subject to a constant stress while approaching their rupture (e.g. Voight 1989, Bevilacqua et al. 2019).

Therefore, under this assumption, the FFM calculates a theoretical time limit for the continuation of the observed nonlinear acceleration, called **failure time**.

Moreover, we studied how such failure time changes as a function of the analyzed data.

Specifically, we compared:

- different GPS stations,
- **baselines** between two stations and **areas** enclosed by three stations.

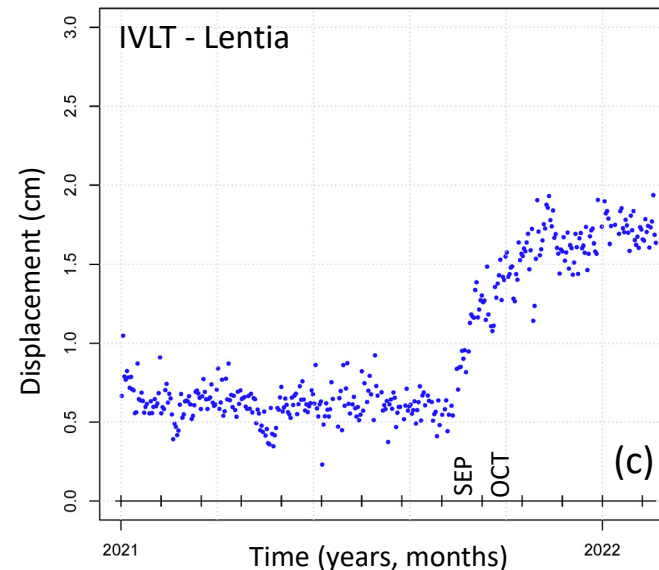
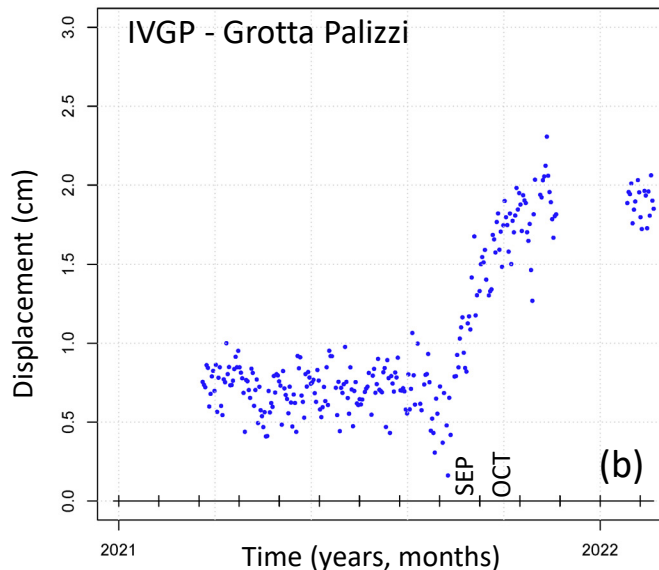
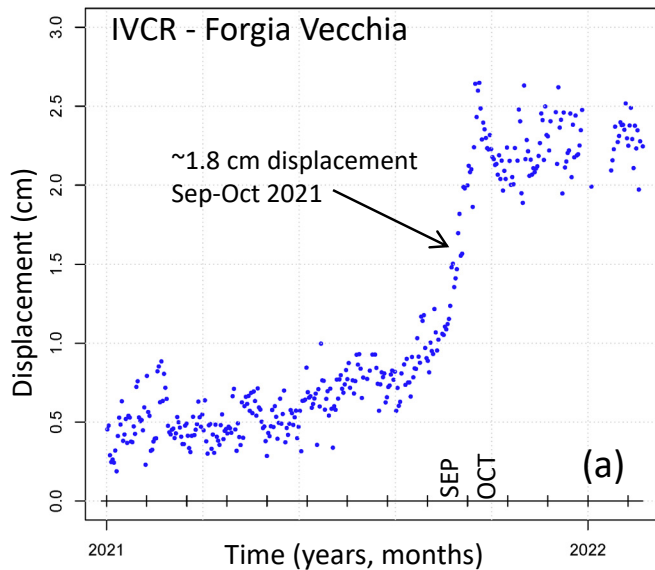
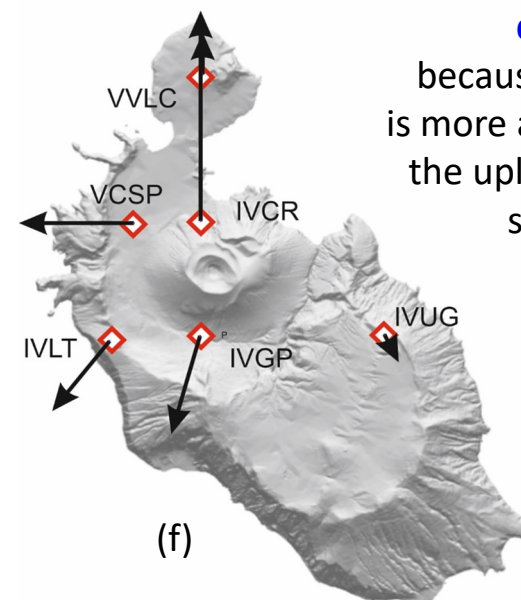
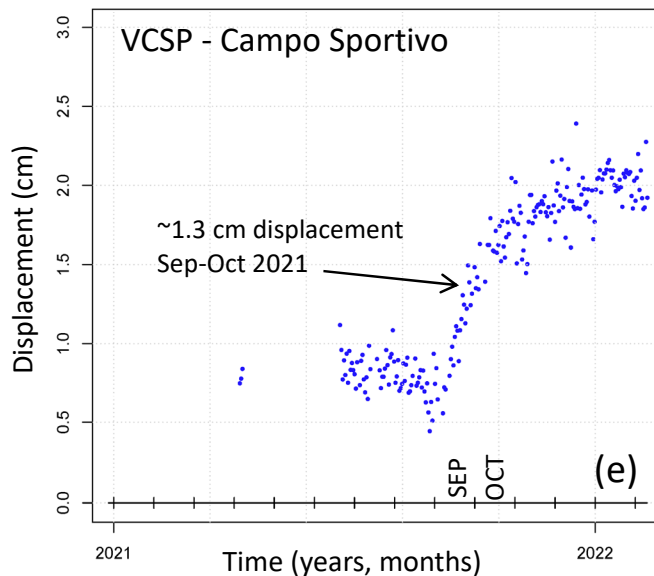
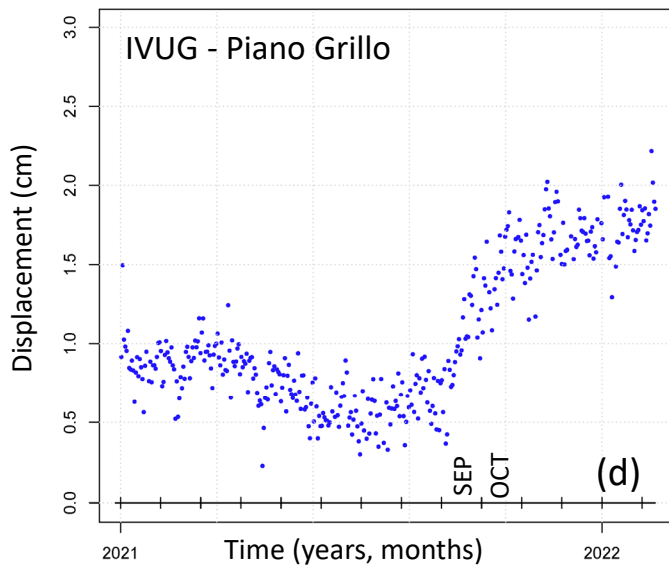


Figure. (a-e) Permanent GPS network, Horizontal ground displacement from 01/2021 to 02/2022. (f) All sites of the permanent GPS stations on Vulcano island.



We focus on **horizontal displacement** because it generally is more accurate than the uplift and shows similar trends.

Baselines and areal dilations

Besides the **horizontal displacement** of single GPS, we studied the **baselines between two GPS** and the **areal extent enclosed by three GPS**.

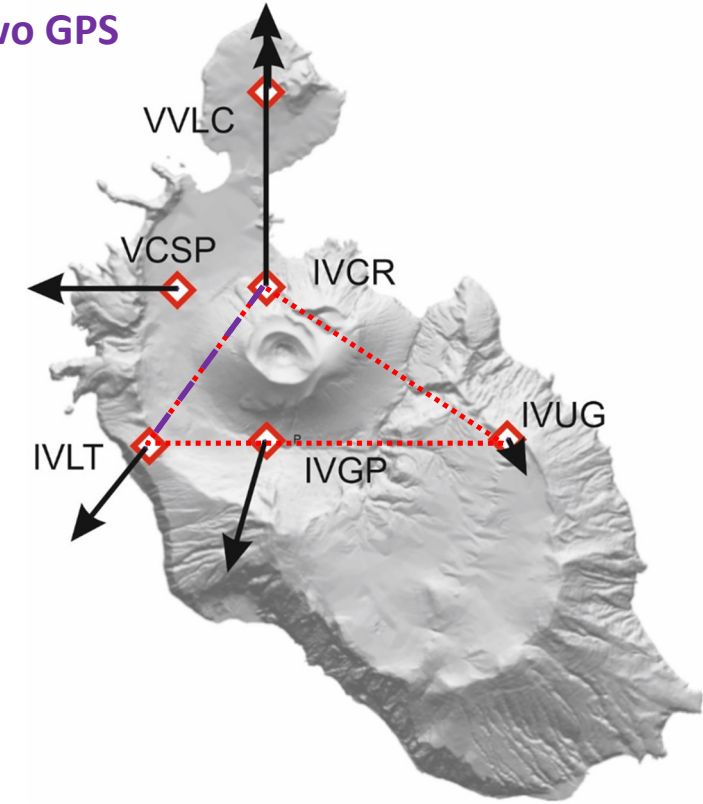
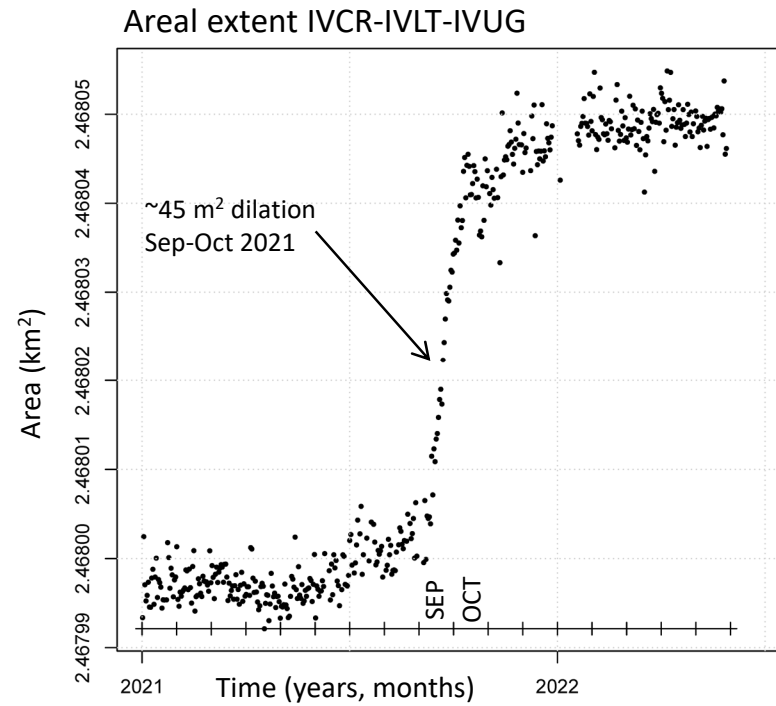
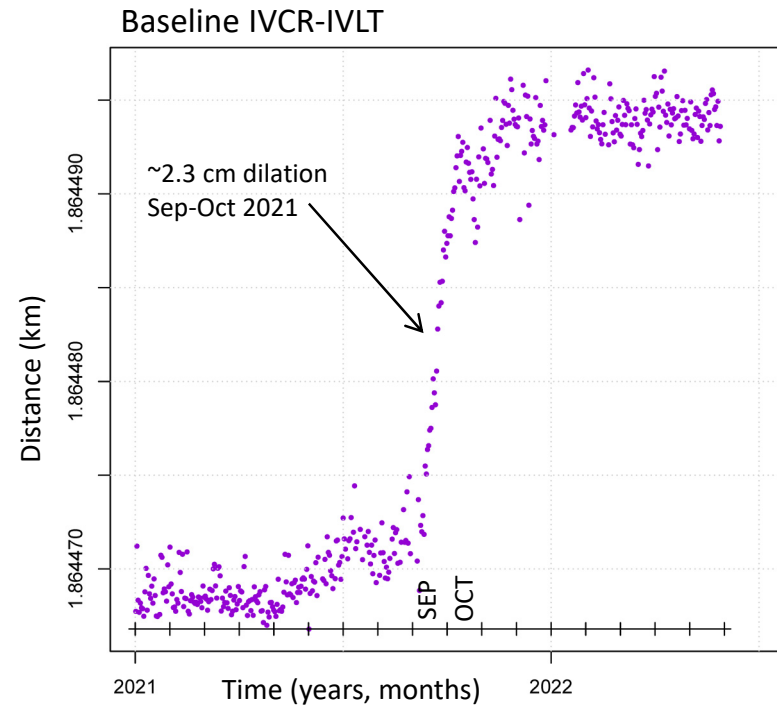


Figure. Permanent GPS network, (a) IVCR-IVLT baseline length and (b) IVCR-IVLT-IVUG areal extent from 01/2021 to 05/2022. (c) Sketch map of the baseline and the triangle analyzed.

IVCR-IVLT
baseline (violet)

IVCR-IVLT-IVUG
triangle (red)

The nonlinear regression model

The FFM assumes the input data as possible precursors, and provides quantitative forecasts through a **nonlinear regression** of their time rate X:

$$dX/dt = AX^\alpha$$

where $A > 0$ and $\alpha \in [1.2, 2.0]$ in our case study (Cornelius and Voight, 1995).
Data fitted

When applying FFM to complex systems in rapid evolution, they may **speed up** and decrease the time left for entering a critical state, or **slow down** and increase it.

However, iterative applications of the FFM can update the time limit by sequentially including new data.

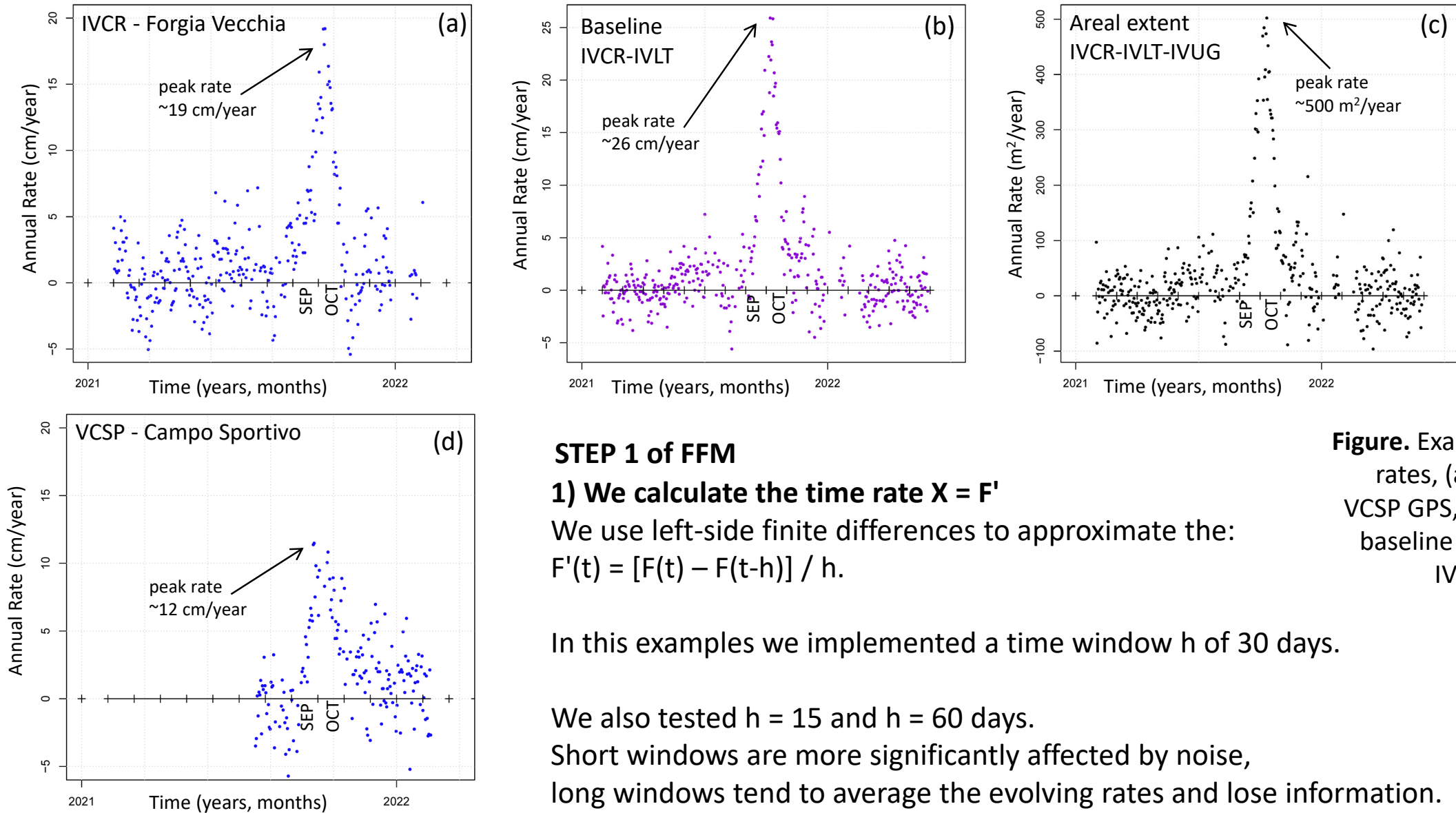
We performed a **daily retrospective analysis** of the temporal evolution of the FFM forecasts, since July 2021.

Our estimates will be expressed in terms of waiting times to reach potentially critical conditions, i.e. we do the **difference between the failure time and the current time**.

We show the mean and the 5th and 95th percentile values due to the uncertainty affecting parameters A, α .

This method enables us to **track waiting times** during the evolving crisis, so to highlight the most critical phases and foresee their possible duration.

STEP 1 - Temporal rates of the signals



STEP 1 of FFM

1) We calculate the time rate $X = F'$

We use left-side finite differences to approximate the:

$$F'(t) = [F(t) - F(t-h)] / h.$$

In this examples we implemented a time window h of 30 days.

We also tested $h = 15$ and $h = 60$ days.

Short windows are more significantly affected by noise,

long windows tend to average the evolving rates and lose information.

Figure. Examples of time rates, (a, d) IVCR and VCSP GPS, (b) IVCR-IVLT baseline and (c) IVCR-IVLT-IVUG area.

STEP 2 - Inverse rates of the signals

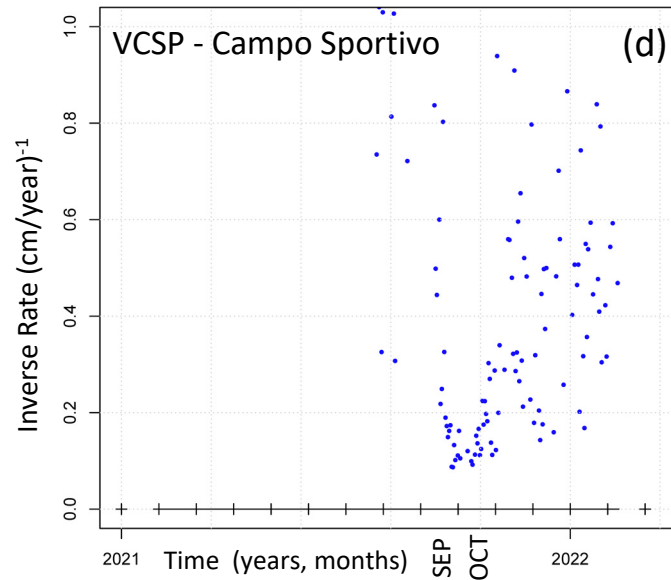
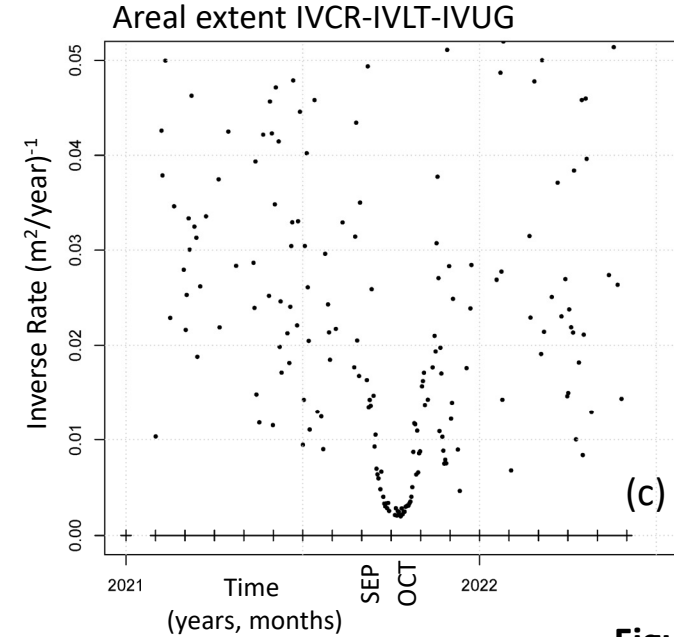
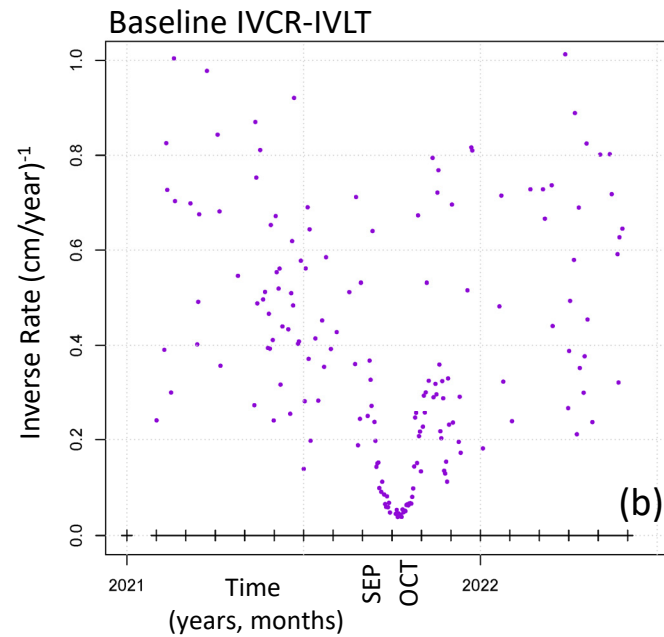
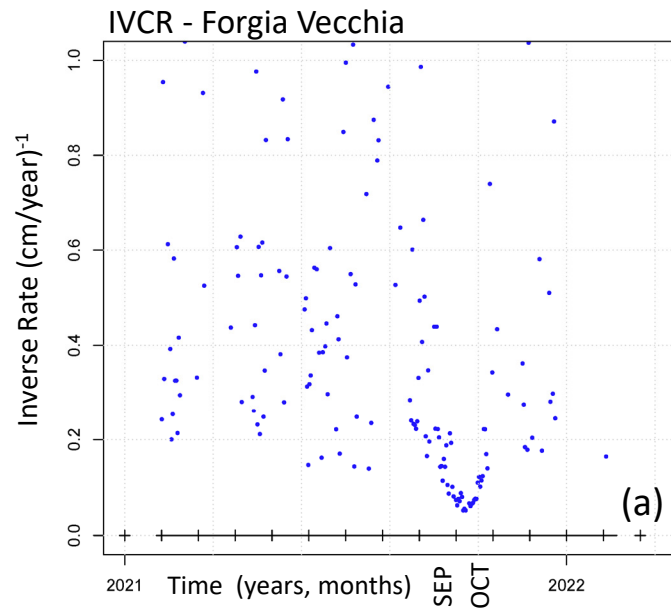


Figure. Examples of inverse rates, (a, d) IVCR and VCSP GPS, (b) IVCR-IVLT baseline and (c) IVCR-IVLT-IVUG area.

STEP 2 of FFM

2) We calculate the positive values of the inverse rate $1/X$
Inverse rates provide a graphic tool to infer the **failure time**.

These examples assume a time window h of 30 days to define X .

If $1/X$ is obtained over short time scales it can become irregular, under a stronger influence of ambient noise. Likewise, $1/X$ is less regular if X is smaller.

STEP 3 - Nonlinear regression

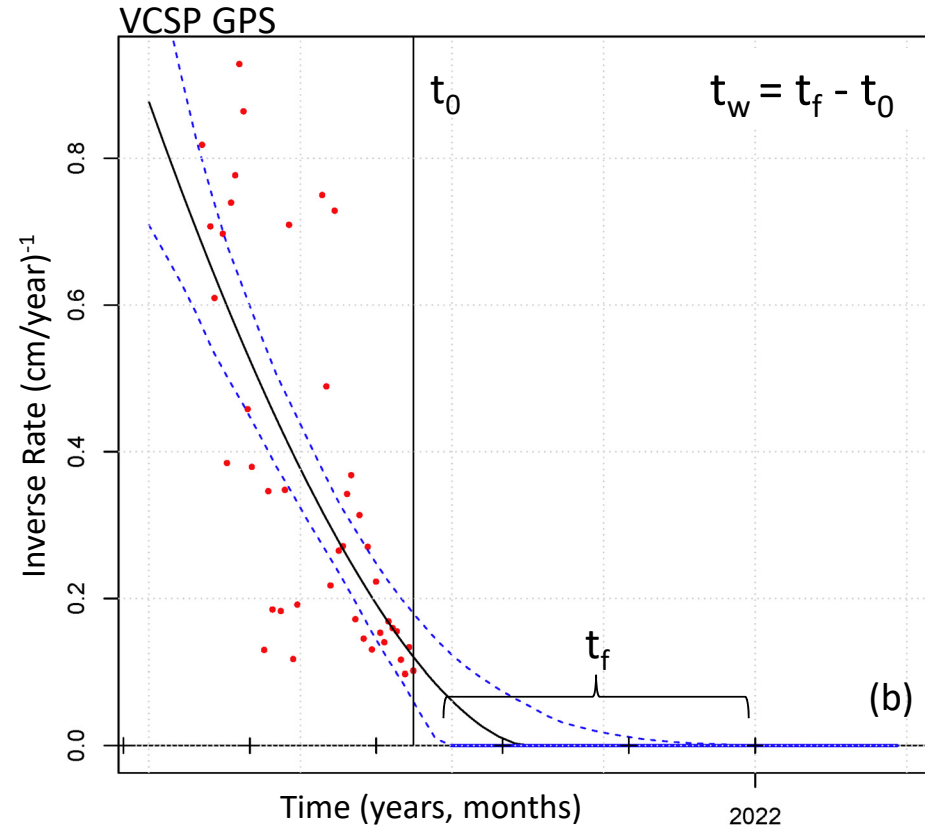
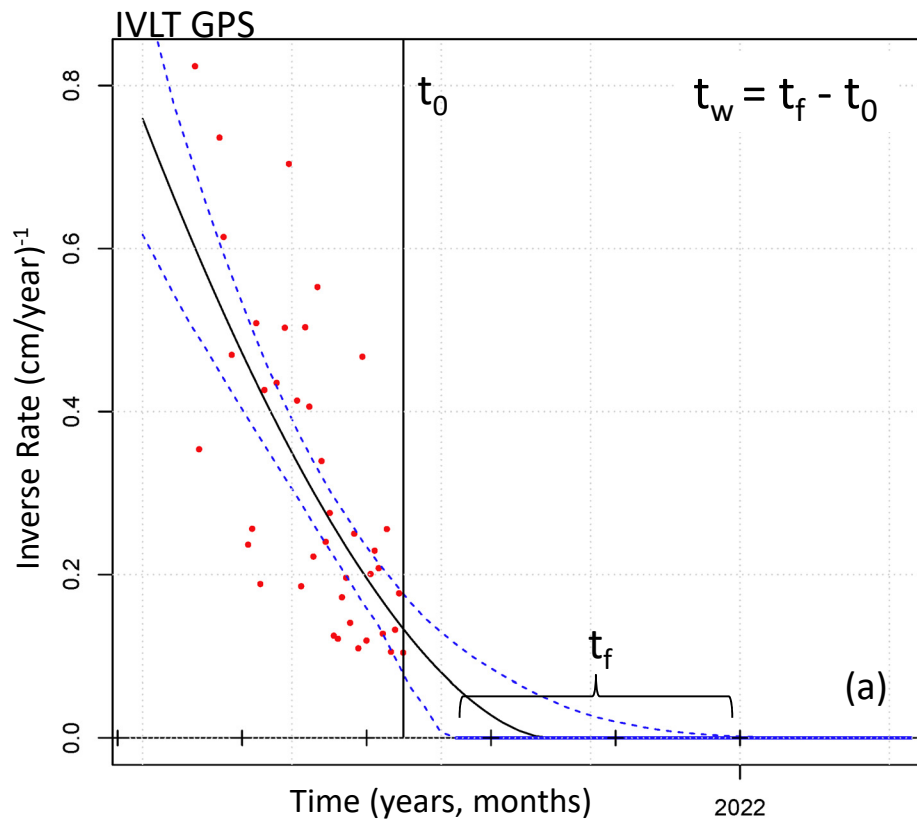


Figure. Examples of FFM nonlinear regression, performed in October 10th 2021.

(a) IVLT GPS, $h = 30$ days,
(b) VCSP GPS, $h = 60$ days.

Red dots are values of $1/X$.

A vertical line marks the current time t_0 .

Blue dashed lines are the 5th and 95th percentile bounds of the regression curve.

STEP 3 of FFM

3) Through nonlinear regression we extrapolate the trend of the positive part of $1/X$

The failure time t_f is defined by the intercept $1/F'(t_f) = 0$.

The waiting time is given by $t_w = t_f - t_0$, where t_0 is the current time. We can consider the waiting time as an **index for the acceleration** of the system, i.e. how close it would be to enter a critical state.

Retrospective analysis, 1-month nonlinear regression

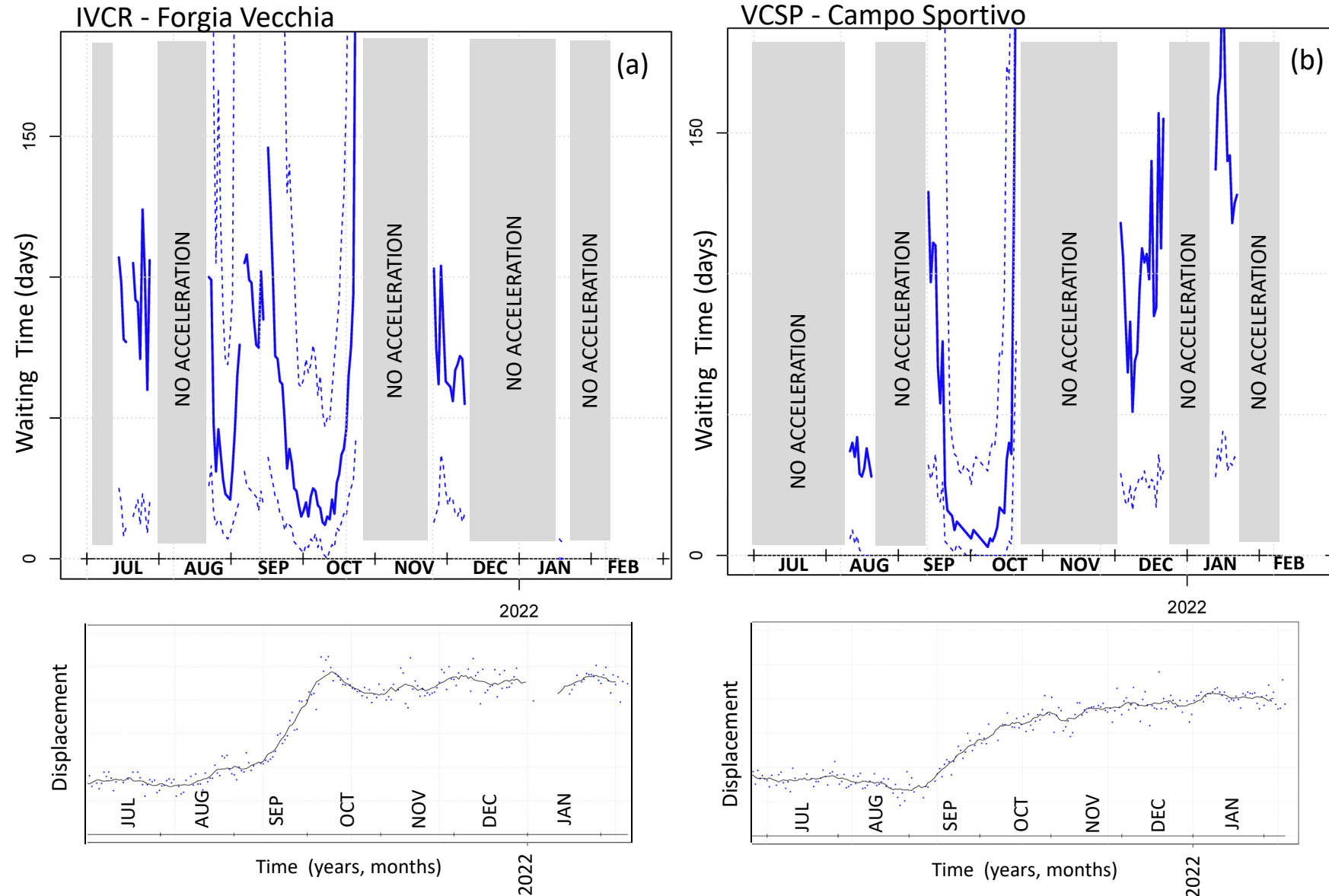


Figure. Retrospective analysis of the waiting time t_w from 07/2021 to 02/2022. Data sources are below, including 10-day moving average. Phases lacking of significant acceleration are marked by grey stripes.

(a) IVCR GPS, (b) VCSP GPS. Dashed lines are the 5th and 95th percentile bounds of t_w .

In Jul and Aug, **weak accelerations** are detected but not synchronous between the two GPS.

A minimum t_w marks the **main acceleration** from mid-Sep to mid-Oct. We obtained t_w less than a week in mean value, **around Oct 10th**.

Afterwards, the index detects a **weak acceleration** from late-Nov (IVCR) to mid-Dec. (VCSP). Another one in mid-Jan.

Retrospective analysis, 2-month nonlinear regression

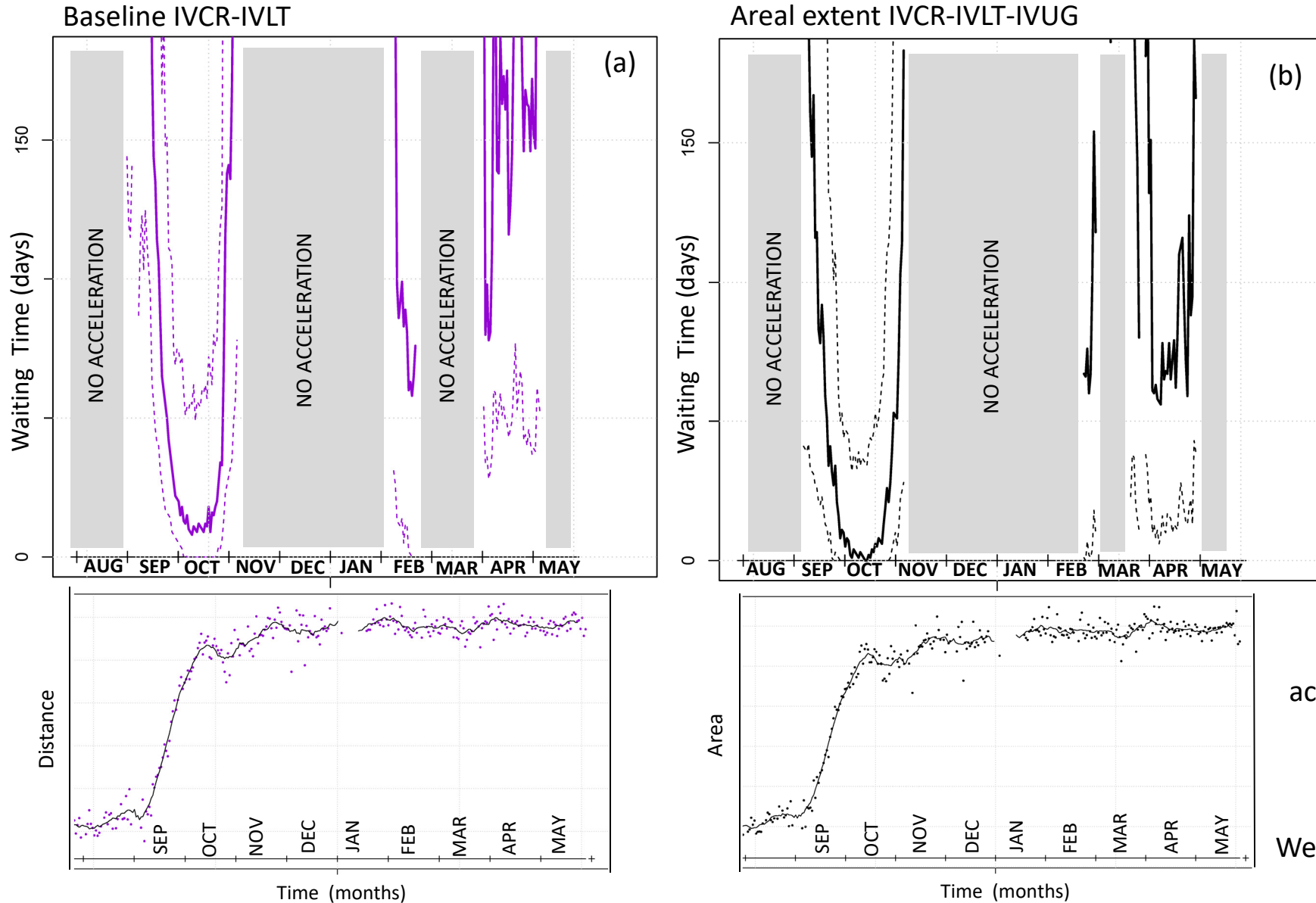


Figure. Retrospective analysis of the waiting time t_w from 08/2021 to 05/2022. Data sources are below , including 10-day moving average.

The phases lacking of significant acceleration are marked by grey stripes.

(a) baseline IVCR-IVLT,
(b) area IVCR-IVLT-IVUG.

Dashed lines are the 5th and 95th percentile bounds of t_w .

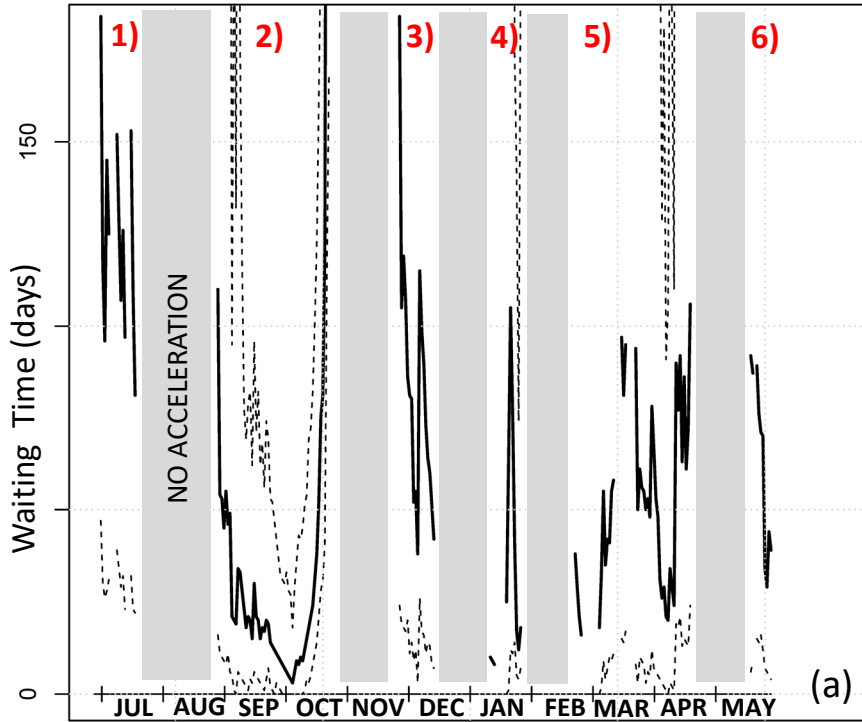
In the 7-months long period from Nov 2021 to May 2022 noise and accelerations are **difficult to distinguish**.

We tested a nonlinear regression **over 2 months**, less sensitive to noise.

We detected phases of weak acceleration in Feb 2022 and Mar-May 2022

Retrospective analysis, 1-month nonlinear regression

Areal extent IVCR-IVLT-IVUG



By comparison, using a nonlinear regression **over 1-month** on the same areal extent data, we detect additional phases of weak acceleration.

In summary we see six phases of acceleration:

1) early to mid-July 2021

2) late-August to mid-October 2021

← the only case with minimum t_w less than 1 week in mean value

3) late-November to mid-December 2021

4) early to late-January 2022

5) late-February to late-April 2022, slowing down in mid-March

← also detected with a 2-month regression

6) mid-May 2022, still ongoing

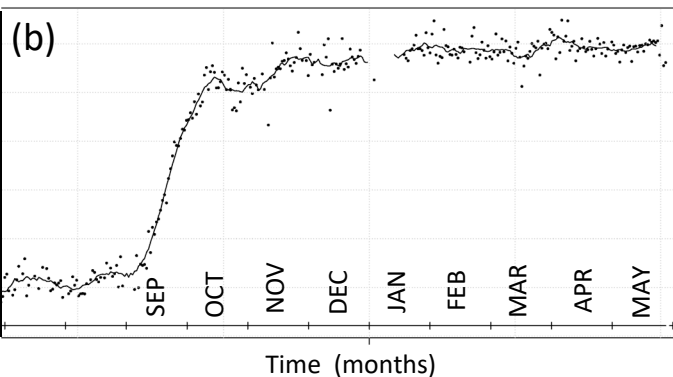


Figure. (a) Retrospective analysis of the waiting time t_w from 07/2021 to 05/2022. (b) data source.

In (a) the phases lacking of significant acceleration are marked by grey stripes. Dashed lines are the 5th and 95th percentiles of t_w .

Mean values of t_w mostly ranged from ~ 25 to 100 days during phases 3-6.

They were greater during phase 1, i.e. ~ 100 to 150 days.

In this study, we analyzed the **temporal rates of GPS data** collected by INGV network on Vulcano Island in 2021-2022, focusing on the mathematical properties of the rapid inflation occurred in September-October and on the 7-month long period afterwards.

In fact, we can see t_w as an **index for the acceleration** of the system, i.e. how close it would be to enter a critical state. We studied how t_w changes as a function of the **different GPS** stations, **baselines** and **areas** defined by multiple stations.

The analysis of IVCR and VCSP GPS showed that a minimum t_w less than a week, **around Oct 10th**, marked the acme of the **main acceleration** from mid-Sep to mid-Oct.

In the 7-months long period from Nov 2021 to May 2022 noise and accelerations are more **difficult to distinguish**. Depending on the length of nonlinear regression implemented, we detected **two to six phases** of weak acceleration.

These phases may be associated with **recurrent pressure increases** in the hydrothermal system.

The described method enabled us to **highlight** the most critical phases and **foresee** their possible **duration**.